

9. Anti-islanding of RE

Two kinds of anti-islanding

When an islanded system occur with balanced RE output and load, and if fault is included in the system, especially the fault is human accident, the islanded system must shutdown as soon as possible. This is the necessity of anti-islanding. It is divided two ways.

Collaboration of System and RE The first way is Collaboration of System and RE. Since both resource of system and RE can be available in the way, high reliability is expected. Three typical examples that have been studied in the world are introduced.

Remote shutdown: Appearance of islanded system is detected at system side. The information is sent to RE. RE stops based on the information. A utility in Japan is eager in realizing the method.

Generation permission signal: Generation permission signal is sent by power line communication. When circuit breaker is tripped by fault, the signal also stops. Thus REs on the faulted distribution line can realize that they must shutdown.

Forced grounding: When circuit breaker is tripped due to distribution line fault, line side of the breaker is forced to grounded in three phases. In islanded system, REs are expected to shut down by their protection system due to the forced grounding.

Cost is calculated taking forced grounding as example. Peak demand of Japan is 180GW, then power flow of a feeder is around 3.6MW. Therefore, number of feeders is calculated as follows.

$$180\text{GW} / 3.6\text{MW} = 50000$$

Forced grounding function must be equipped on at most 50000 circuit breakers. Additional cost for the function is assumed 1 million yen for 1 breaker. Total cost is at most calculated as follows.

$$50000 \text{ breakers} * 1 \text{ million yen} / \text{breaker} = 50,000 \text{ million yen}$$

The cost is quite smaller than battery for RE output storage. The reason of “at most” is, it is not necessary to replace all breakers at a time, but breakers can be replaced at timing when need of replace occurs. Removed breakers can be reused in another feeder. In 20 years, all breaker will be replaced.

In most developed countries, anti-islanding is not now taken into grid code, may be taken into grid code in near future. Then, collaboration of system and RE is recognized as hopeful in those countries, and now field test of forced grounding is going⁽¹⁾⁽²⁾.

Detection at RE side only The second way is detection at RE side. Anti-islanding is performed by only RE side. However, the detection is not easy, therefore, reliability is inferior to the collaboration way. Who claims the second way as standard is Japan only among developed countries. Two methodologies exist in the second way.

Passive methods: The methods presume islanding by value and varying speed of measured physical variables at RE. They are called as “islanding detection”, but the reality is “abnormal variable detection”, and it was recognized that probability of mal-detection and miss-detection is rather high from the beginning of development. Especially “phase jump” has been preferred by high sensitivity, but resulted many mal-detection. In network fault, RE trips due to anti-islanding in many scene where RE should continue operation by FRT function. Thus, FRT function is spoiled very much.

Active methods: The method uses signal poured by RE into network, and was once hoped more reliable than

passive methods. However, it was recognized that poured signal from many REs interfere each other and detection sensitivity decreases.

Thus in Japan, even knowing (or they may not knew) that reliability is inferior than the first way, the second way has become standard. The author deduces the reason as follows. (This is only deduction. No proof exist.) In early stage of RE integration, electric power companies burdened a difficulty that anti-islanding must be performed by RE only so that high RE integration is interfered. Electric equipment makers welcomed anti-islanding as non-tariff trade barrier.

Further, another deduction as follows is possible. One of the collaboration way, forced grounding must be equipped only when it becomes necessary, and need not being equipped in all breakers. On the contrary, in case of the second way, all REs must equip the function from the beginning. In other words, intending that cost of anti-islanding is increased and advanced, the second way was chosen. Initiative of establishing grid code was taken by distribution section, which had close connection with sales section for a long time, and it is quite natural that those sections had tendency to prevent RE integration.

Frequency feedback method with step injection

Although RE were burdened such heavy problem, an active method, “slip mode frequency shift” method was developed by a bender. The method has evolved to the title method by preparing “step injection ” to shorten islanding detection time, and is now expected as the most promising active method. However, physics of anti-islanding seems to be very difficult to understand, unreasonable explanations have been invented and are now flowing. Therefore they are here corrected first.

Structure as shown in Fig. 9.1 is assumed. Inverter is regarded as current source I_{inv} . Load is expressed as paralleled resistance R , inductance L , and capacitance C . Power system is modeled as voltage source V_{sys} . Output of inverter and load power are just balanced, and they are isolated from power system.

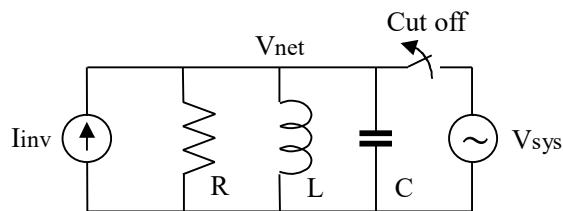


Fig. 9.1 Structure for islanded inverter and load

Origin of the method that detects frequency shift as input and outputs reactive power shift has character shown in Fig. 9.2(3). As shown as “inverter character”, when of network voltage V_{net} frequency exceeds by Δf_{net} rated frequency, IGBT gate is controlled so that inverter current I_{inv} phase lead by $\Delta\phi_{inv}$ than network voltage V_{net} phase.

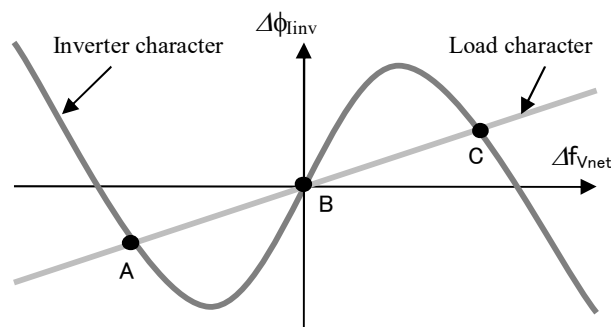


Fig. 9.2 Principle of slip mode frequency shift

As to the load, if frequency rises, capacitance’s effect exceeds inductance’s effect, so current phase leads. On the contrary when frequency drops, inductance’s effect exceeds capacitance’s effect, so current phase lags. As the results, load characteristics shown in the figure is conducted.

When interconnected, Inverter leads current phase with frequency rise, but when islanded, network voltage phase leads together with inverter current phase, so inverter must lead current phase more and more. Thus, increase of phase by time, that is, frequency rises, ant reaches point C in the figure. On the contrary, when frequency drops,

operation goes to point A. A and C is stable equilibrium, but B is unstable equilibrium. Apart from B very small, gate control operates to apart more. Thus at last, operation reaches A or C, that is, slightly apart from rated frequency, therefore, islanding can be detected by frequency deviation. While interconnected, network voltage frequency does not change even if inverter current phase changes.

Explanation above is added only a little words to Ref. (3). The explanation is easy to understand, because reference is written to be understood easily. On the contrary, Ref (4) is explain as follows. Can readers understand? ... “In case that total power factor of load combined with resistance is lagging, just after switch off, inverter that is performing current control will operate so that voltage phase leads to maintain current phase up to now”... Inverter does not have function to control voltage phase, does it? Since voltage phase leads as result, it must be described what is how controlled to reach the result.

Aside from explanation, the method is attractive because islanding is well detected even if many inverters are included in the islanded system. However, if generation and consumption of active and reactive power are very well balanced in the islanded system, a little time delay will occur for islanding detection. As countermeasure, Ref. (4) confirms when islanding is doubted, it is effective to generate step change of inverter current phase by simulation and experiment.

Following it, the method is recommended in Ref (5) as “new type active method”, but the explanation is written as follows. Can readers understand? ... “The method detects frequency deviation rate, and detects islanding fast by sharply injecting reactive power so that frequency deviation is amplified.”... In islanded system, since only loads exist outside of inverters, reactive power injection cannot realize physically without varying voltage and frequency. Also, although the explanation assumes that reactive power is the cause and frequency is the result, it seems quite difficult to explain how the cause-result relation is generated.

But the way, the method seems to be promising. In Ref. (4), it is confirmed that the method is available when induction motor load exists in the islanded system. It is regard as practical that passive methods that were suffered from mal-operation should not use for tripping but should be used for giving trigger for the step injection in the method.

Impact on oscillatory stability⁽⁷⁾

Analysis method of oscillatory stability including RE’s anti-islanding is already introduced in chapter 6. Here, one typical power sending system (Sen.) and one typical power receiving system are picked up among Japan interconnection, aggregated into one machine one load infinite bus system, and examined. Structure of those system is already shown in Fig. 6.2 Parameters are shown in Table 9.1. If generator power exceeds 90% of its capacity, capacity is increased to power/0.9.

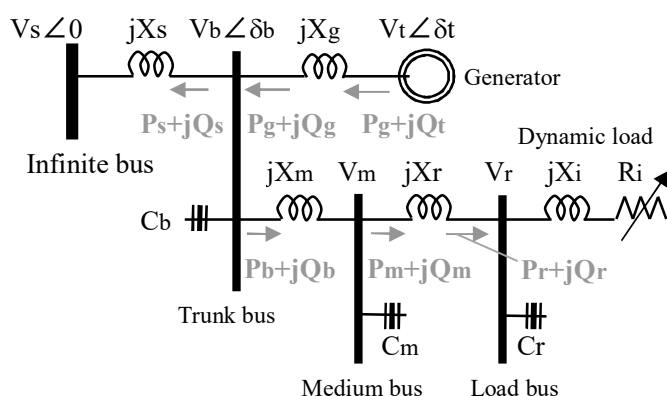


Fig. 6.2(again) Model for oscillatory stability analysis

Load’s voltage sensitivity is different at system bus (b), medium bus (m), and load bus (r), also is different in stationary (Stat) and transient (Tran) condition. Those sensitivities excluding capacitor connecting to the bus is shown in Table 9.2. Stationary β_b shows very large negative value due to large amount of capacitor at medium bus.

Table 9.1 Parameters of the systems (basic case)

	G _{cap}	V _t	P _g	X _g	V _b	X _s	X _m	V _m
Sen	1	1.03	0.7565	0.2058	1	3.2302	0.3591	1
Sen RE	0.7249	1.03	0.5484	0.2627	1	3.2302	0.3591	1
Rec	1	1.03	0.8172	0.2812	1	1.3167	0.1125	1
Rec RE	0.5316	1.03	0.4344	0.4134	1	1.3167	0.1125	1

	X _r	PL	PRE	C _b	C _m	V _r
Sen	0.2701	0.6937	0	0.0060	0.2992	0.9613
Sen RE	0.2701	0.6937	0.2081	-0.0266	0.2265	0.9594
Rec	0.1204	1.2760	0	0.2319	0.4294	0.9716
Rec RE	0.1204	1.2760	0.3828	0.1648	0.3569	0.9684

Table 9.2 Load's voltage sensitivity

Case		α_b	β_b	α_m	β_m	α_r	β_r
Sen	Stat	1.362	-7.746	1.083	-0.014	1	0
	Tran	2	2	2	2	2	2
noRE	Stat	1.255	-10.66	1.074	0.217	1	0.375
	Tran	2.392	4.031	2.437	2.089	2.429	1.625
Rec	Stat	1.171	-9.907	1.06	-0.013	1	0
	Tran	2	2	2	2	2	2
RE	Stat	1.137	-14.93	1.056	0.237	1	0.375
	Tran	2.425	3.946	2.439	2.032	2.429	1.625

Table 9.3 Generator constants (machine capacity base)

M	X _d	X _{d'}	X _{d''}	T _{d'}	T _{d''}	X _q	X _{q'}	X _{q''}	T _{q'}	T _{q''}
7.00	1.75	0.30	0.23	1.00	0.03	1.70	0.55	0.23	0.30	0.03

Same generator and excitation system is adopted in sending and receiving systems. Generator constants are shown in Table 9.3. Saturation is not modeled. Design of excitation system is shown in Fig. 9.3. Here, T_e is exciter's time constant, which is 1.0sec in case of usual rotating exciter and 0.1sec in case of for thyristor exciter. ΔP type PSS, which has very common constants and is not tune up, is modeled. RE's reactive power is -0.2 times of its active power⁽⁸⁾.

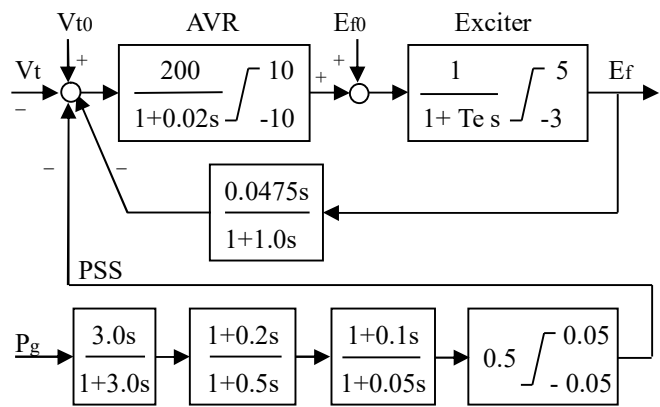


Fig. 9.3 Design of excitation system

Power sending system Tie line flow is 0.0628 in Table 9.1 condition.. Varying generator output by 0.01 step, Nyquist' trajectories are drawn. Those without and with anti-islanding cases are shown in Fig. 9.4 and 9.5.

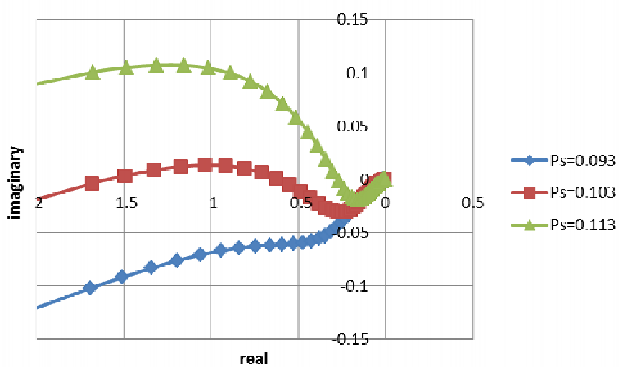


Fig. 9.4 Nyquist' trajectory (Sen. w/o a-isl.)

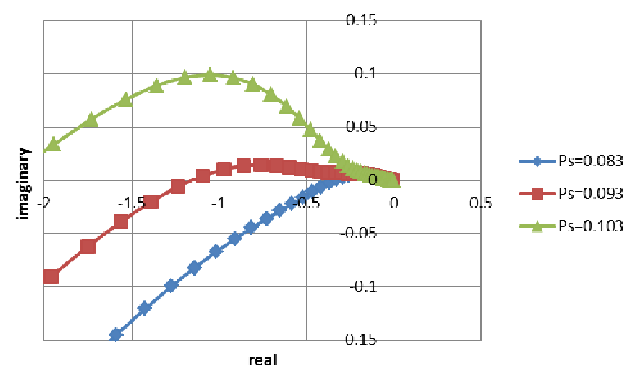


Fig. 9.5 Nyquist's trajectory (Sen. With a-isl)

Stability limit is obtained from Nyquist's trajectory. When a point on the trajectory become closest to point (-1, 0), swing frequency f and distance from the point d are obtained. In stable case, d is converted to $-d$. Thus Fig. 9.6 is obtained for Fig. 9.4 case. Damping is well as d shows large negative value. Several data of (P_s , d) and (P_s , f) are

approximated by parabolic curve. When d is zero, it is found that critical sending flow is 0.101 and swing frequency is 0.490Hz.

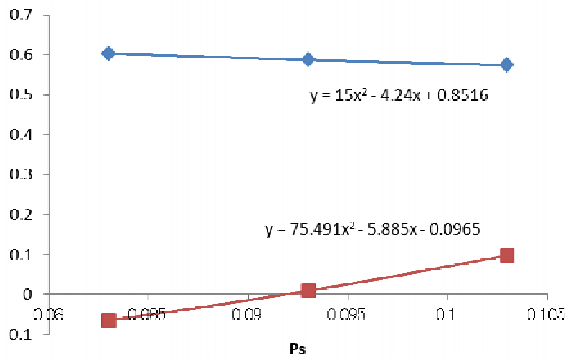


Fig. 9.6 Swing frequency and damping (Sen. w/o a-isl)

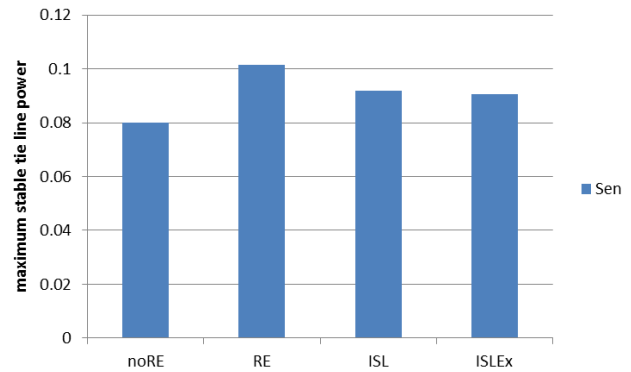


Fig. 9.7 Maximum stable tie line power flow (Sen.)

Thus, in four cases: no-RE, with RE, with RE and anti-islanding (ISL), and with RE, anti-islanding, and fast excitation system (ISLEx), maximum stable tie line sending power are compared as Fig. 9.7. In sending system stability limit in “with RE and anti-islanding” case is not lower than that of no RE case, the issue is not serious. Fast excitation system does not show significant success. The reason is thought that optimal resetting of PSS is not performed.

Power receiving system Tie line flow is 0.4588 in table 9.1 condition. By varying generator power by 0.05 step, Nyquist’s trajectories are drawn. Those without and with anti-islanding cases are shown in Fig. 9.4 and 9.5.

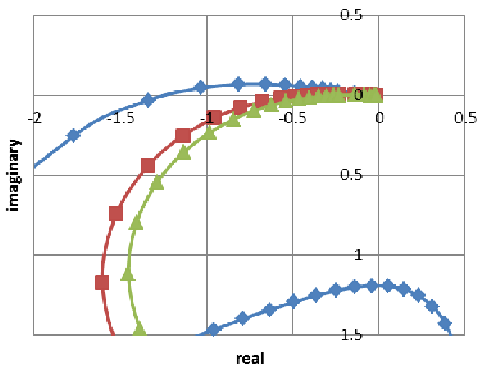


Fig. 9.8 Nyquist’s trajectory (Rec. w/o a-isl)

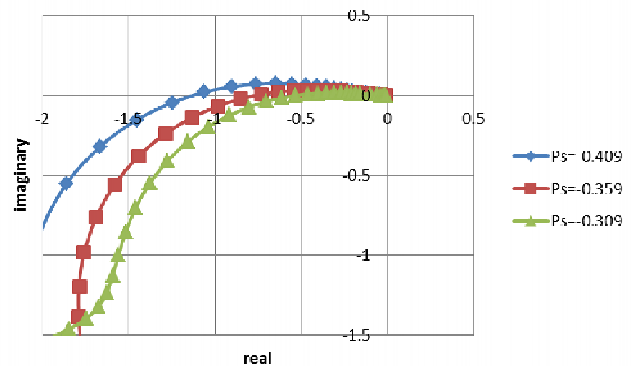


Fig. 9.9 Nyquist’s trajectory (Rec. with a-isl)

Damping by tie line flow in “with RE” case is shown in Fig. 9.10. Several data are approximated by parabolic curve. When damping d is zero, it is found that tie line receiving flow is 0.599 and swing frequency is 1.573Hz.

Minimum stable tie line (sending) flow in the four cases is compared in Fig. 9.11. Case with anti-islanding (ISL) shows much poorer oscillatory stability than case without anti-islanding (RE) case, and further poorer than no RE case. As improving method, fast excitation

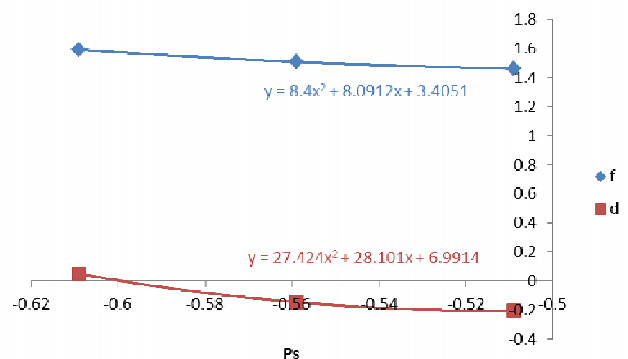


Fig. 9.10 Swing frequency and damping (Rec. w/o a-isl)

system is quite effective.

Study By K-coefficients in block diagram system stability can be presumed. In unstable cases, at least one K-coefficient is negative.

K-coefficients in unstable cases in sending system is shown in Table 9.4. Instability in sending system is usual instability with negative K5, which appears consistently in no RE, with RE, and with anti-islanding cases. Therefore, the instability is caused by synchronous generator and excitation system, impacts of RE and anti-islanding is small.

Table 9.4 K-coefficients in unstable cases (Sen.)

Case		K1	K2	K3	K4	K5	K6
noRE	K0	0.133	1.761	0.981	0.443	-0.094	1.536
	Ps=0.093	K'	0.173	1.207	1.906	0.371	-0.041
RE	K0	0.136	0.990	1.111	0.589	-0.119	1.245
	Ps=0.113	K'	0.145	0.926	2.149	0.459	-0.061
ISL	K0	0.167	0.928	1.142	0.572	-0.086	1.197
	Ps=0.093	K'	0.170	0.902	2.156	0.473	-0.044

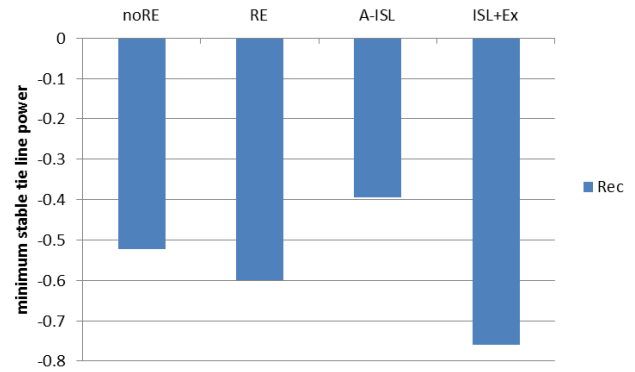


Fig. 9.11 Minimum stable tie line (sending) flow (Rec.)

Table 9.5 K-coefficients in unstable cases (Rec.)

Case		K1	K2	K3	K4	K5	K6
noRE	K0	1.284	4.195	-1.348	-0.251	0.917	4.101
	Ps=-0.559	K'	0.676	1.671	2.457	0.665	0.162
RE	K0	0.681	1.421	-4.648	-1.910	1.470	4.306
	Ps=-0.609	K'	0.485	0.880	3.096	0.888	0.221
ISL	K0	0.549	1.312	0.680	0.670	0.349	2.022
	Ps=-0.409	K'	0.474	0.937	2.960	1.122	0.084

K-connection in unstable cases in receiving system is shown in Table 9.4. Instability in receiving system is an unique phenomenon with negative K3 (and K4), which appears in stationary term of no RE and with RE cases, but does not appear in with anti-islanding case. The reason is that synchronous generator is sufficiently stable due to small receiving flow but anti-islanding is so severe to spoils the stability totally.

Thus, it is understand that most serious case is with anti-islanding in receiving system. Gain-frequency response of damping coefficient D's real part including impact by anti-islanding is examined as shown in Fig. 9.12. Profile is not much different in sending and receiving systems. Real part of D rapidly decreases if swing frequency exceeds 0.4Hz and goes negative. Filter of anti-islanding introduces the character.

Factors in Reduction of damping coefficient due to anti-islanding D_{ISL} without band pass filter (BPF)

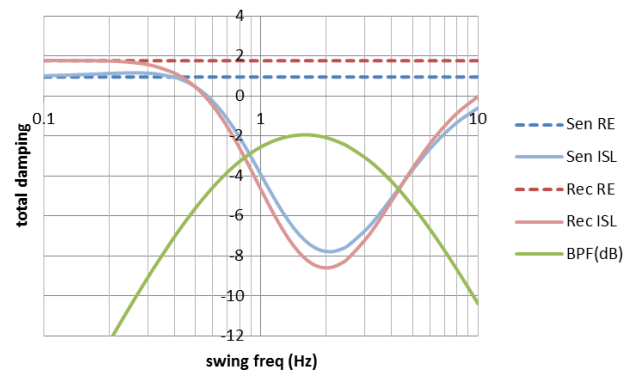


Fig. 9.12 Frequency response of total daping

Table 9.6 Reduction of damping due to anti-islanding D_{ISL}

Case		Δf_r	ΔQ_{RE}	ΔV_r	ΔP_r	l	Total
		$\Delta \omega$	Δf_r	ΔQ_{RE}	ΔV_r	W_g	
Sen ISL	Stat	0.553	-6.24	1.423	0.506	1.380	-3.43
	Tran				1.756		-11.9
Rec ISL	Stat	0.269	-11.5	1.087	0.922	1.858	-5.76
	Tran				2.240		-14.0

character in both systems are compared in Table 9.6. $\Delta f/\Delta\omega$ is larger in sending system. $1/W_g$ is larger in receiving system. As the result, product of all factors (Total) D_{ISL} is not much different in sending and receiving systems.

Therefore, the reason why decline of oscillatory stability due to anti-islanding is remarkably appears in receiving system is difference in swing period. Power swing in sending system is caused by negative K_5 and around 0.5Hz speed. Power swing in receiving system is unique phenomenon with negative K_3 and has 1.0Hz or more speed.

Frequency response of PSS gain's real part considering anti-islanding is shown in Fig. 9.13, in which also influence of band pass filter (BPF) character is seen. Gain decreases at 1.0Hz speed or faster in both system but not so significant, so impact is not much.

Therefore as to the impact by anti-islanding, major problem is that reactive power injection results voltage change and load power change that spoils system damping, and the problem becomes more serious in receiving system whose power swing is fast than in sending system.

There is a possibility to mitigate the decline of oscillatory stability by changing filter character in anti-islanding. For trial, lead time constant (HPF) is changed from 0.2 sec to 0.1 sec, lag time constant (LPF) ins changed from 0.05sec to 0.025sec. Frequency response of damping's real part considering anti-islanding is shown 9.14. Swing speed at which damping begins to reduce shifts to fast side. Therefore, impact of anti-islanding on oscillatory stability can be mitigated by redesign of filter.

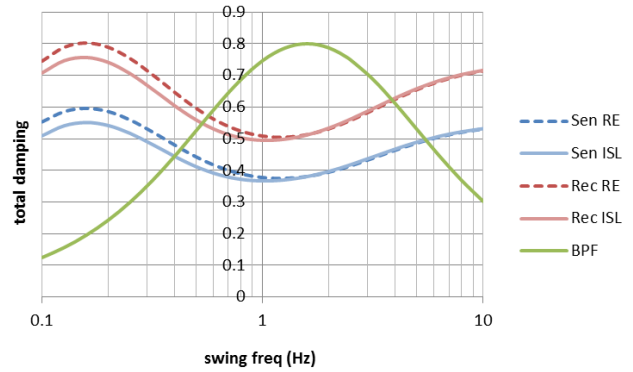


Fig. 9.13 Frequency response of PSS gain's real part

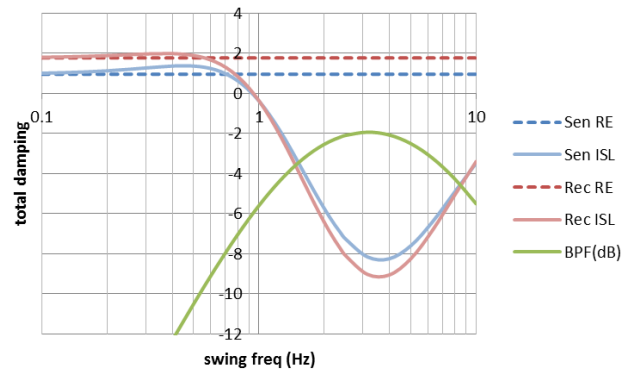


Fig. 9.14 Total damping (shifts to fast side)

Simulation

Analysis (by hand) is instructive to understand phenomenon, but is so rough calculation that it does not suit to identify stability limit accurately. It is simulation that suit for the purpose.

Anti-islanding is modeled as combination of high impedance rotary condenser having constants as shown in Table 9.6 and special excitation system as shown in 9.15. These model structure has been used from the beginning of simulation. Due to the high impedance, machine has very poor voltage support ability.

Fig. 9.6 Constants of rotary condenser for anti-islanding

M	Xd	Xd'	Xd''	Td'	Td''	Xq	Xq'	Xq''	Tq'	Tq''	Xl
0.2	4.0	3.35	3.25	0.2	0.02	4.0	3.35	3.25	0.2	0.02	3.2

As fault a three-phase-to-ground is given through 5.0 p.u. reactance and cleared after 0.1 sec so that good S/N ratio is kept and variation remain within linear area. Depth of instantaneous voltage sag due to fault is 12%

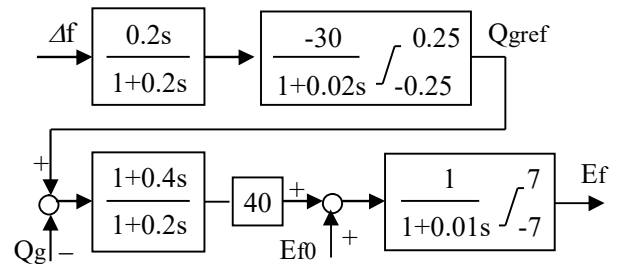


Fig. 9.15 Excitation system for anti-islanding

or less.

Sending system Frequency deviation at load bus is shown in Fig. 9.16 (without anti-islanding) and Fig. 9.17 (with anti-islanding).

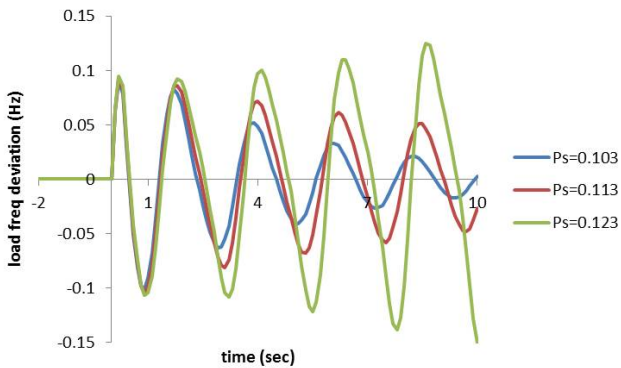


Fig. 9.16 Frequency deviation (Sen. w/o anti-islanding)

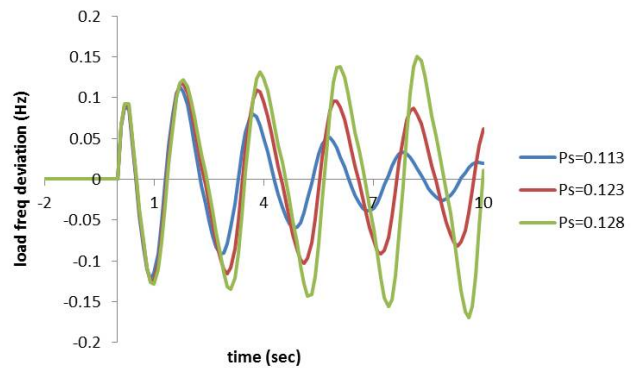


Fig. 9.17 Frequency deviation (Sen. With anti-islanding)

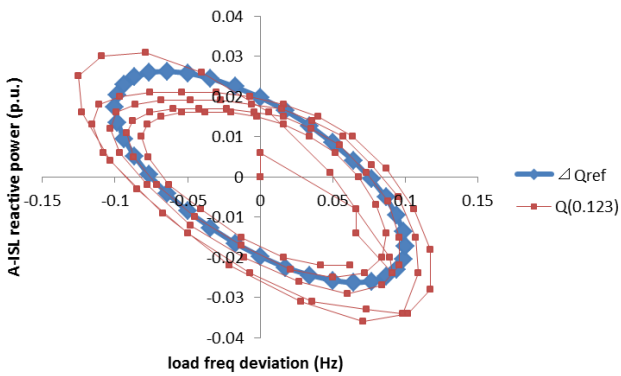


Fig. 9.18 Designed and measured f-Q Lissajour (Sen.)

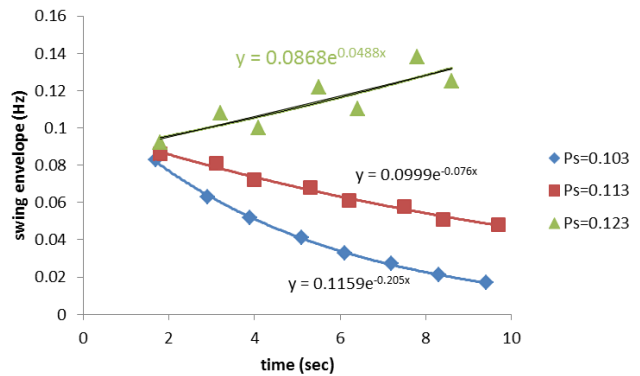


Fig. 9.19 Index function approximation of swing magnitude (Sen.)

Fig. 9.18 shows f-Q Lissajour of anti-islanding simulated in Fig. 9.17. Designed value calculated from gain and filter can represents the simulation result.

Fig. 9.19 is plots of absolute value of frequency deviation peak and bottom in Fig. 9.16, by which growth or shrink speed of frequency deviation, and tie line power flow that gives just zero growth. That is stability limit.

Stability limit of each case is shown in Fig. 9.20. The case that anti-islanding is modeled as rotary condenser but does not operate (RC) shows very little better stability than RE without anti-islanding case. The difference is negligible small.

In the figure answers by analysis are also shown. Analyses give pessimistic assessments. In simulation results, harm of anti-islanding does not appear in sending system.

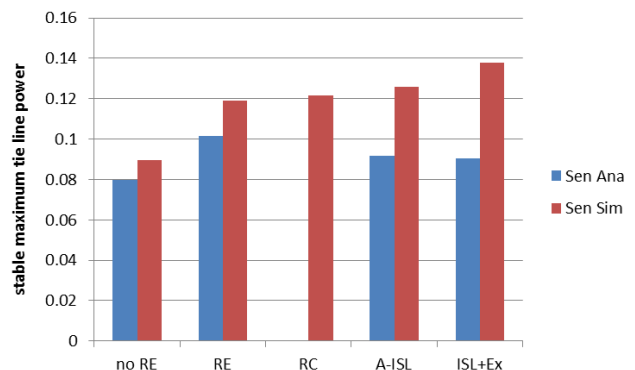


Fig. 9.20 Maximum stable tie line sending power (Sen.)

Receiving system Frequency deviation at load bus is shown in Fig. 9.21 (without anti-islanding) and Fig. 9.22 (with anti-islanding).

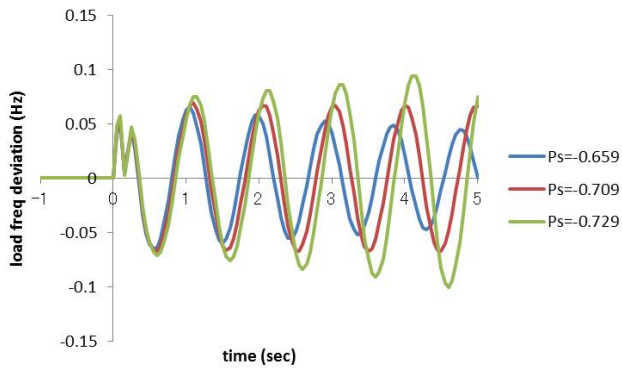


Fig. 9.21 Frequency deviation (Rec. w/o anti-islanding)

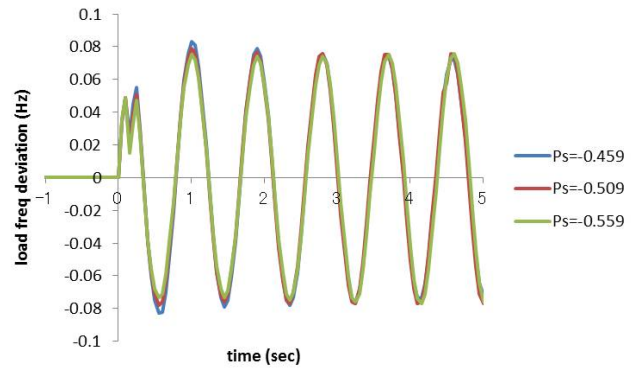


Fig. 9.22 Frequency deviation (Rec. with anti-islanding)

Fig. 9.23 shows f-Q Lissajour of anti-islanding simulated in Fig. 9.22 Q(-0.509). Designed value calculated from gain and filter can represents the simulation result.

Fig. 9.24 is plots of absolute value of frequency deviation peak and bottom in Fig. 9.21, by which growth or shrink speed of frequency deviation, and tie line power flow that gives just zero growth. That is stability limit.

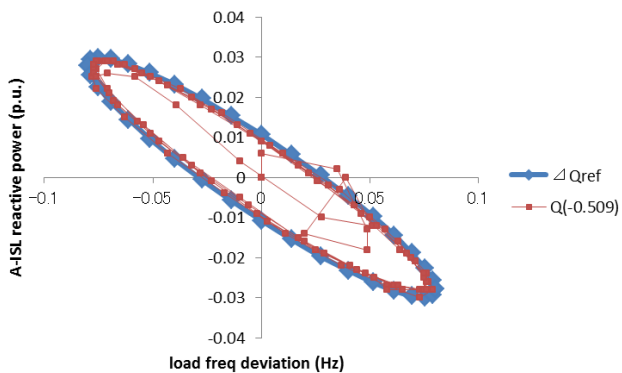


Fig. 9.23 Designed and measured f-Q Lissajour (Rec.)

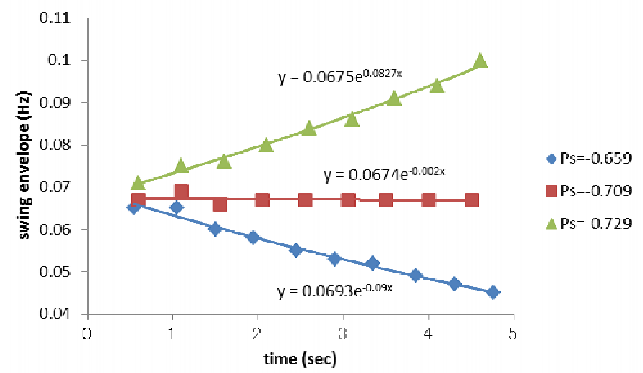


Fig. 9.24 Index function approximation of swing magnitude (Rec.)

Stability limit of each case is shown in Fig. 9.25. The case that anti-islanding is modeled as rotary condenser but does not operate (RC) shows very little better stability than RE without anti-islanding case. The difference is negligible small.

In the figure answers by analysis are also shown. Analyses give pessimistic assessments. In analysis and simulation results, harm of anti-islanding is considerably large, but can be mitigated by adopting fast excitation system such as thyristor type considerably.

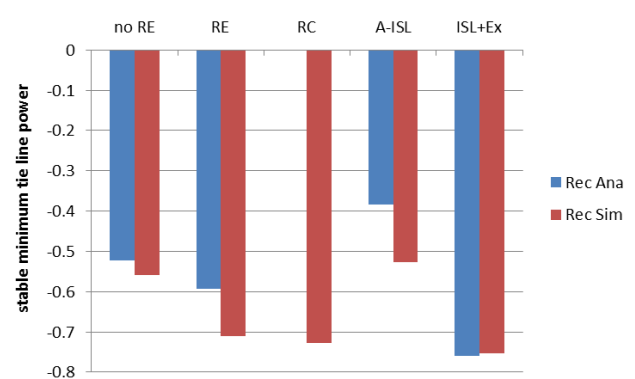


Fig. 9.25 Minimum stable tie line sending power (Rec.)

Growing swing in receiving system occurs by Demello's coefficient K3 and K4 going negative. Growing swing in islanded power system occurs by K3 and K6 going to negative. The both occur as hunting on loop control: flux => voltage => flux without passing rotor. This is the reason that swing growth speed does not vary by tie line power flow in Fig. 9.22. Rather design of excitation system becomes dominant. Therefore, high speed excitation system is

effective.

Summary It was found that origin of anti-islanding’s harm on oscillatory stability is that frequency deviation changes load’s consuming power, which equivalently reduce generator’s damping coefficient, and make negative. Reduction of PSS effect is not zero but is not much.

Analyzed cases are verified by simulation. Totally saying, analyses give pessimistic assessments than simulation. The reason is thought that pessimistic parameters were adopted. Since the analyses is pessimistic, is available for screening.

In power sending system with long power swing period impact of anti-islanding does not become serious. However, power swing in receiving system has short period, and filter character also affects, anti-islanding has considerable impact.

In existing power system, many (local) receiving systems appear. There, aged thermal generators are replaced, and then, fast excitation system such as thyristor type is adopted. Therefore, the impact is hoped to be considerably mitigated in existing power system, but must be once assessed. If mitigation is insufficient, there is some room of improvement by changing filter character in anti-islanding.

Hunting of anti-islanding itself⁽⁹⁾

It was so called “voltage flicker” phenomenon that first appeared as instability when high PV integration became reality. Although no faults occurred, cyclic voltage deviation around 7Hz appeared. The phenomenon is instability on closed loop constructed by “frequency feedback” type anti-islanding. If expressing mechanism, calling as “hunting” is more suitable because it hits the nail head . However, calling “flicker” is suitable to explain phenomenon, and is not a mistake.

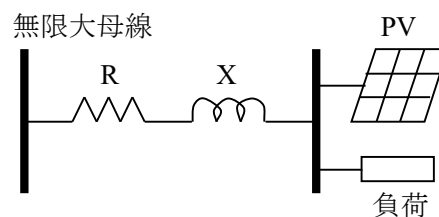


Fig. 9.26 Structure of model system

Power system model that can deal hunting by “frequency feedback” most simply is shown in Fig. 9.26. Block diagram explaining the hunting phenomenon is shown in Fig. 9.27.

Tr means high pass filter. If frequency detection time span is 0.2sec, Tr is also 0.2sec.

G is anti-islanding gain. If 25% reactive power of rated capacity in 0.5Hz deviation, the gain is calculated as

$$G = \frac{-0.25}{0.5\text{Hz} / 60\text{Hz}} = -30 \text{ p.u.}$$

Here, lagging reactive power is expressed as positive value.

Td is a lagging time constant modeling moving average. Moving average during 0.04sec is expressed the half Td: 0.02 sec.

Th is a small delay time constant mentioned after. Here, it is zero.

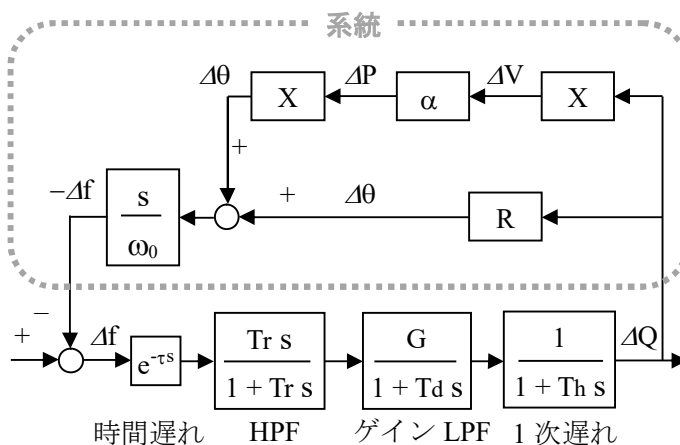


Fig. 9.27 Block diagram explaining hunting phenomenon

R is resistance seen from PV to infinite bus. As shown in Fig. 9.28, by lagging reactive power increase ΔQ , voltage vector varies during Δt from initial value $V(0) = 1$ to $V(\Delta t) = 1 - j R \Delta Q$. Then, phase varies approximately $\Delta\theta \doteq -RQ$ (rad).

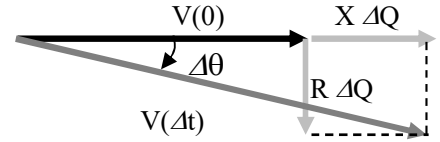


Fig. 9.28 Reactibe power and V phase

X is reactance seen from PV to infinite bus. By increase of lagging reactive power ΔQ , voltage of PV and load rises by $X \Delta Q$. Then, by difference between PV's and load's voltage sensitivities α , receiving current increases by $\Delta P = \alpha X \Delta Q$, and voltage phase of PV and load lags by $\Delta\theta = X \Delta P$

To such a fast deviation as hunting PV cannot follow by MPPT, but operates in ACR control (seen as constant current), and load is seen as constant impedance because motor cannot vary speed so fast. Therefore, if PV operates at rated power and is well balanced to load, difference of PV's and load's voltage sensitivity is $\alpha = 2 \cdot 1 \text{p.u.} - 1 \cdot 1 \text{p.u.} = 1 \text{p.u.}$

Thus, voltage phase lags affected by both R and X. Frequency is time differential phase. Here, as system rated frequency is expressed as 1 p.u., divided by $\omega_0 = 120\pi$ to make dimension agree as follows.

$$\Delta f = \frac{1}{\omega_0} \frac{d\theta}{dt}$$

Thus generated frequency rise Δf forms a feedback system as Fig. 9.27. Open loop gain of the system is expressed as follows.

$$A = e^{-\tau s} \frac{Tr s}{1 + Tr s} \frac{G}{1 + Td s} (R + \alpha X^2) \frac{s}{\omega_0}$$

Since differential exists in power system side, the gain never decline at high frequency, and time delay joins, absolute value of open loop gain at high frequency must be less than 1 as follows for keeping the system stable.

$$|A_H| = \left| \frac{G (R + \alpha X^2)}{Td \omega_0} \right| < 1$$

By parameters above: $G = -30$, $a = 1$, $Td = 0.02$, $\omega_0 = 120\pi$, the stable condition is expressed as follows.

$$|A_H| = \frac{30 (R + X^2)}{0.02 \times 120\pi} < -1$$

Instability occurs in condition as follows and Fig. 9.29. Per unit method is PV capacity base.

$$R + X^2 > \frac{0.02 \times 120\pi}{30} \doteq 0.25$$

In case that PV is partial output, that (collected) load locates at midst of (collected) PV and infinite bus, equivalent α is obtained by Y-connection aggregation.

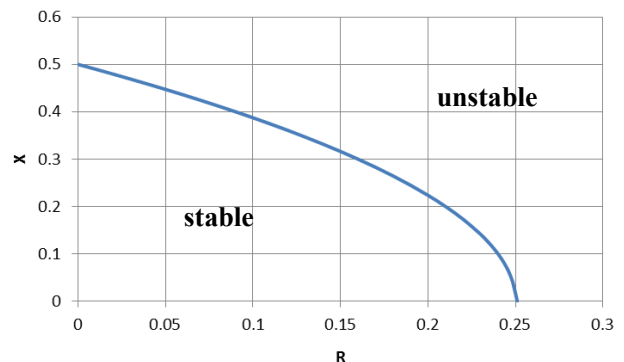


Fig. 9.29 Boundary of hunting appearance

(The reason shall be thought by reader.)

Here as stabilizing measure, small lagging (time constant T_h in Fig. 9.27) is added to reduce open loop gain at high frequency. The effect cannot be shown as Fig. 9.29, but expressed by Nyquist's trajectory. Condition: $\tau = 0.015$, $R = 0.2$, $X = 0.4$, $a = 1$ is assumed. By neglecting time delay in frequency detection, Nyquist's trajectory is drawn as Fig. 9.30. In $T_h = 0$ case, trajectory is drawn as circle at high frequency, in $T_h = 0.02\text{sec}$ case, gain at high frequency declines, the former circle shrinks, and the system is stabilized.

Since the hunting phenomenon is a proof of side effect of "anti-islanding by RE side only", which is forced by electric utilities as obstruction, it seems very shameful to report to government, utilities and benders are making countermeasure secretly. Such concealment is not favorable, the author informed in Ref. (9).

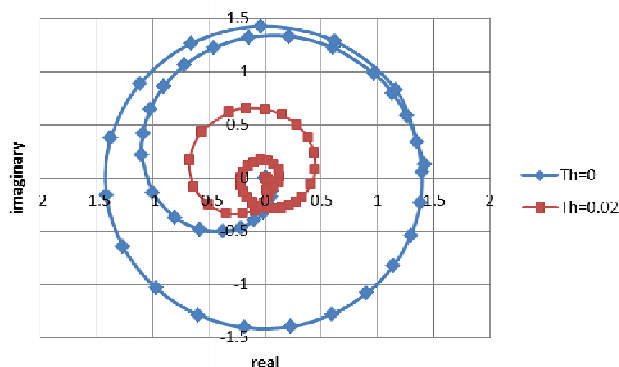


図 9.30 Nyquist 軌跡

References

- (1) W. Wang, J. Kilber, G. Zhang, W. Xu, B. Howell, T. Palladino: "A Power Line Signaling Based Scheme for Anti-Islanding Protection of Distributed Generators – Part 2: Field Test Results", IEEE Trans. PWRD, Vol.22, No.3, pp.1767-1772 Jul. 2007
- (2) C. Abbey, Y. Brissette, P. Venne: "An Autoground System for Anti-Islanding Protection of Distributed Generation", IEEE Trans PWRD, Vol.29, No.2, pp.873-880, Mar. 2014
- (3) Y. Noro, H. Shinohara, T. Kasai, C. Okatsuchi, and Y. Sato* "Development of an Islanding Protection System That Operates Fast without Interference", IEEJ Proc. PE, No. PE-10-9 (2010)
- (4) New Energy Developing Organization Report: "Establishment of Detecting Technique of Islanding", Aug. 2009
- (5) The Japan Electric Association: "Grid Interconnection Code JEAC 9701-2010 [2011Revised Addition 1]" (2011)
- (6) S. Uemura, M. Tagagi, and K. Kawahara: "Preventing Islanding by Distributed Power Generation at Transmission System Fault-Evaluation of Characteristics of Detecting Islanding by Power Conditioning Subsystem for Interconnecting Many Distributed Power Generations in Area with Rotated Type Distributed Power Generation", CRIEPI Report, No. 12020 (2013)
- (7) S. Komami, T. Sakata, and S. Yamada: "Impact of RE's Anti-Islanding on Power System Oscillatory Stability", IEEJ Trans. PE, Vol. 136, No. 6, pp.557-568 (2016)
- (8) M. Ishimaru, H. Tamachi, and S. Komami: "Positive Effect of PV's Constant Leading Power Factor Operation in Power System", IEEJ Trans. PE, Vol. 132, No. 7, pp.615-622 (2012)
- (9) N. Kanao and S. Komami: "Mechanism and Countermeasure of Hunting caused by Anti-Islanding Scheme using Frequency-feedback Method of Photovoltaic Generation", IEEJ Trans. PE, Vol. 137, No.7, pp.546-554 (2017)